



A Novel Dual Lattice Discrete Particle Model for Multiphysics Simulation of Coupled Mechanical and Transport Behavior in Concrete Members Subjected to Long-term Loading

Dongge Jia

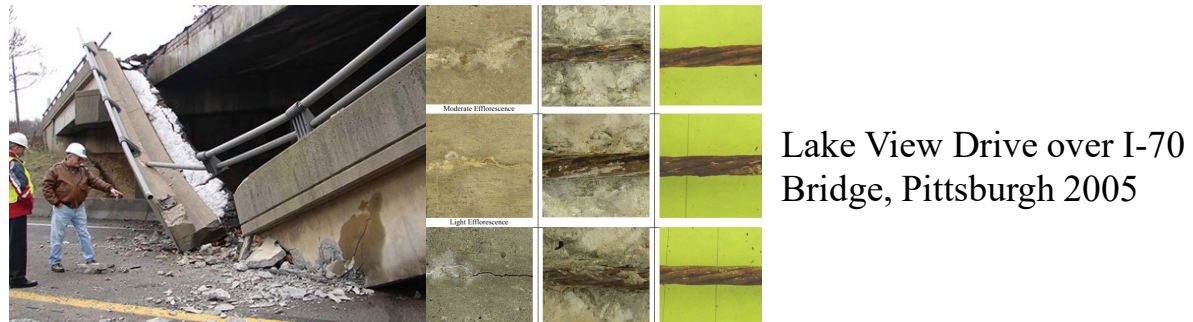
Authors: Dongge Jia, Yingbo Zhu, John C. Brigham, Alessandro Fascati

Department of Civil and Environmental Engineering

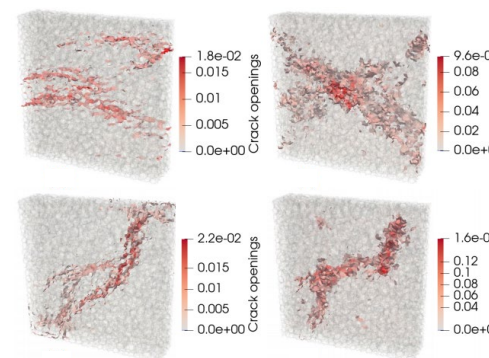
Department of Bioengineering

Background and Motivation

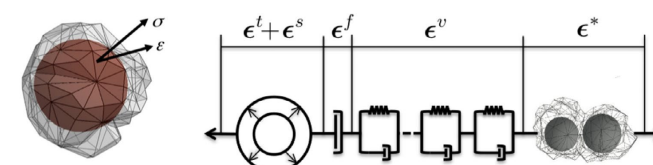
- Chloride-induced corrosion in concrete members is a major reason for deterioration of civil infrastructure.
- Corrosion is a temporal multiphysics process involving concrete damage and chloride intrusion.
- Modeling methods exist to simulate concrete fracture, chloride transport, and concrete creep, but comprehensive and efficient methods to model the meso-scale interaction between crack paths, chloride flow, and load-induced viscous strain do not exist.



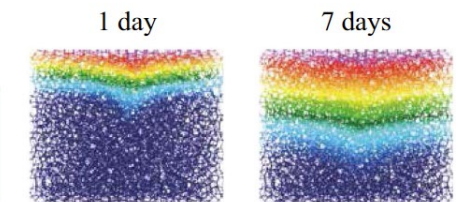
Lattice discrete particle modeling (LDPM) of concrete fracture (Jia et al. 2024)



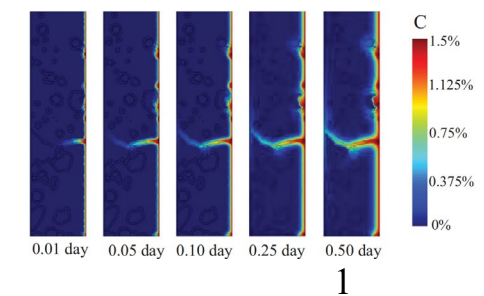
Integrating creep and shrinkage behavior into LDPM (Mohammed et al. 2019)



LDPM of chloride invasion (Antonio et al. 2023)



FEM of chloride invasion (Qiu and Dai 2021)



Research Objective and Innovation

The goal of this research is to:

- (1) Build a computational tool using lattice discrete particle modeling (LDPM) to simulate concrete corrosion subjected to long-term loading and presence of deicing chloride.
- (2) Apply the computational tool to assess and interpret the meso-scale interaction between crack patterns, chloride transport, and the creep effect.

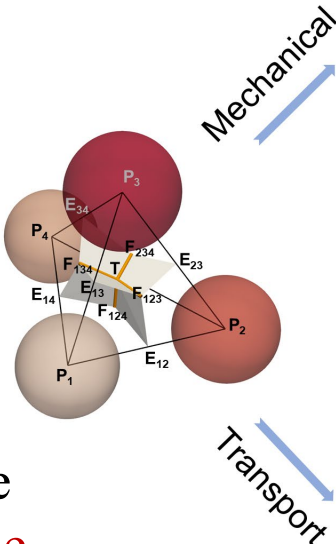
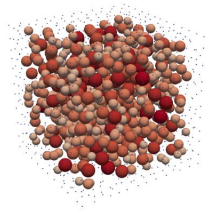
The dual LDPM advantages:

- (1) A meso-scale physical representation of crack width and corresponding chloride transport.
- (2) Consideration of unsaturated conditions by separating water convection and chloride diffusion.
- (3) Consideration of concrete creep for structures under long-term loading.

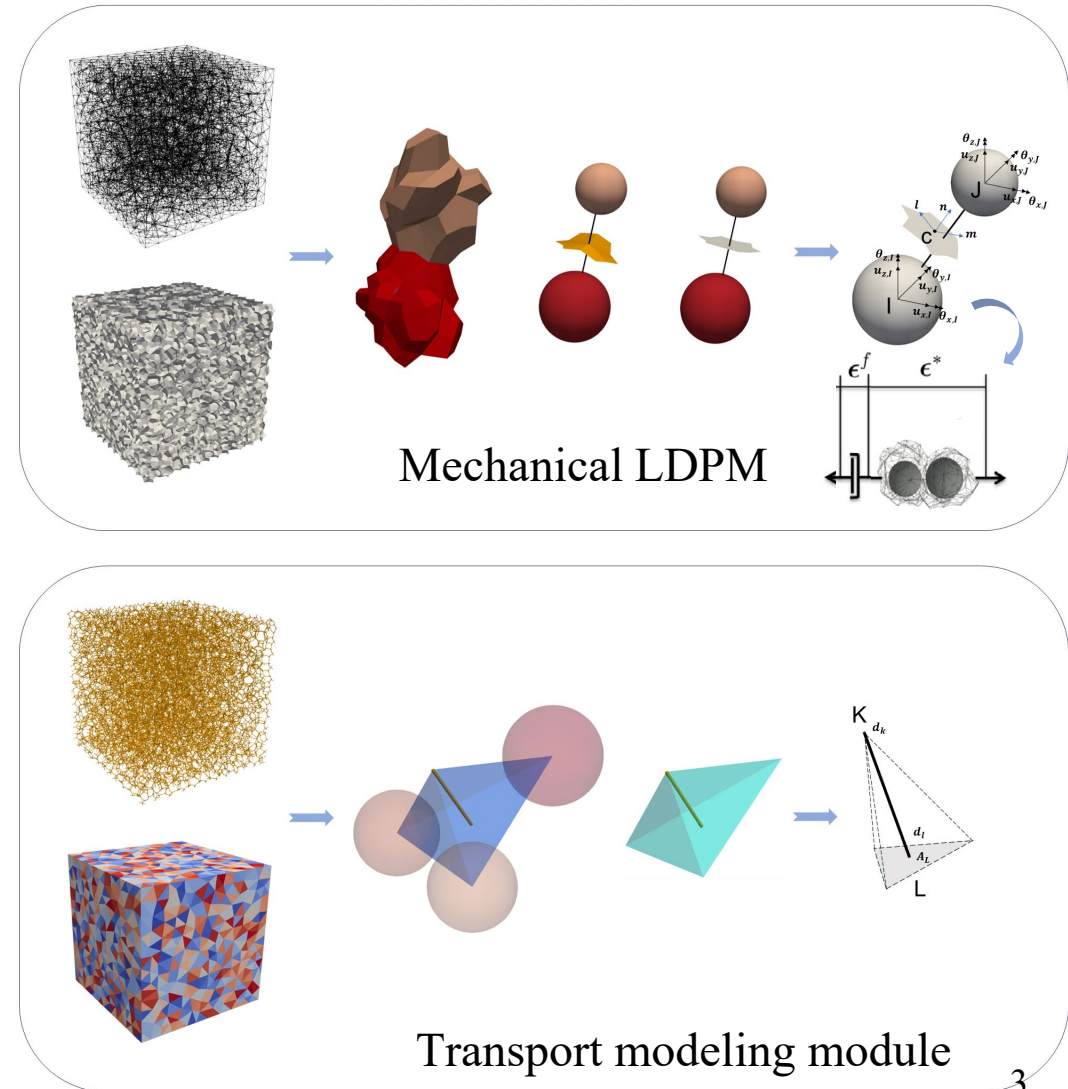
Dual LDPM Framework

Additions to the standard LDPM framework:

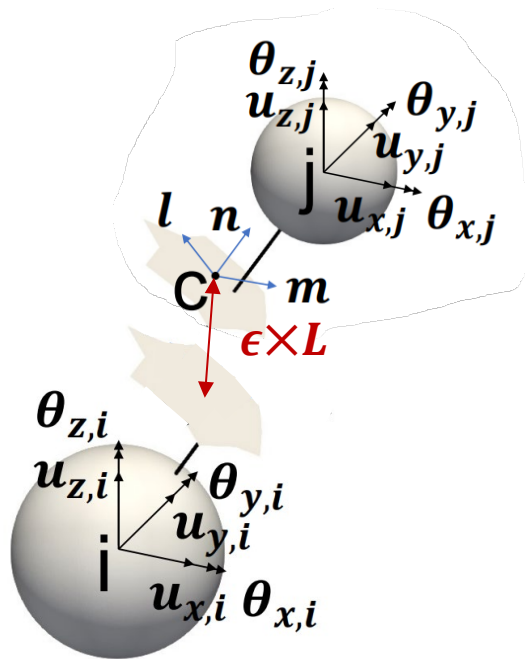
- (1) **Concrete creep** is introduced by embedding a viscous strain into the composition of facet strains.



- (2) **Transport elements** are created on the edges of LDPM tessellation **where the cracking occurs**.



LDPM for Concrete Fracture with Creep Effect



Nodal degrees of freedom and facet strain of a lattice element

Governing equation

$$\nabla^2 \sigma = 0$$

Discrete strain compatibility and force equilibrium equations

A displacement jump is transformed into facet strains:

$$\varepsilon_{Nk} = \frac{\mathbf{n}_k^T [\![\mathbf{u}_{Ck}]\!]}{\ell_e} = \mathbf{B}_N^{jk} \mathbf{Q}_j - \mathbf{B}_N^{ik} \mathbf{Q}_i$$

$$\varepsilon_{Mk} = \frac{\mathbf{m}_k^T [\![\mathbf{u}_{Ck}]\!]}{\ell_e} = \mathbf{B}_M^{jk} \mathbf{Q}_j - \mathbf{B}_M^{ik} \mathbf{Q}_i$$

$$\varepsilon_{Lk} = \frac{\mathbf{l}_k^T [\![\mathbf{u}_{Ck}]\!]}{\ell_e} = \mathbf{B}_L^{jk} \mathbf{Q}_j - \mathbf{B}_L^{ik} \mathbf{Q}_i$$

The nodal forces at nodes i and j associated with facet k are:

$$\mathbf{F}_{ik}^T = -\ell_e A_k (\sigma_{Nk} \mathbf{B}_N^{ik} + \sigma_{Mk} \mathbf{B}_M^{ik} + \sigma_{Lk} \mathbf{B}_L^{ik})$$

$$\mathbf{F}_{ik}^T = \ell_e A_k (\sigma_{Nk} \mathbf{B}_N^{kj} + \sigma_{Mk} \mathbf{B}_M^{kj} + \sigma_{Lk} \mathbf{B}_L^{kj})$$

Summing up the nodal forces at all nodes and equating it to the external force provides the LDPM equilibrium equations.

LDPM for Concrete Fracture with Creep Effect (cont.)

Constitutive law

$$\dot{\varepsilon}_\alpha = \dot{\varepsilon}_{\alpha,ed} + \dot{\varepsilon}_{\alpha,v}$$

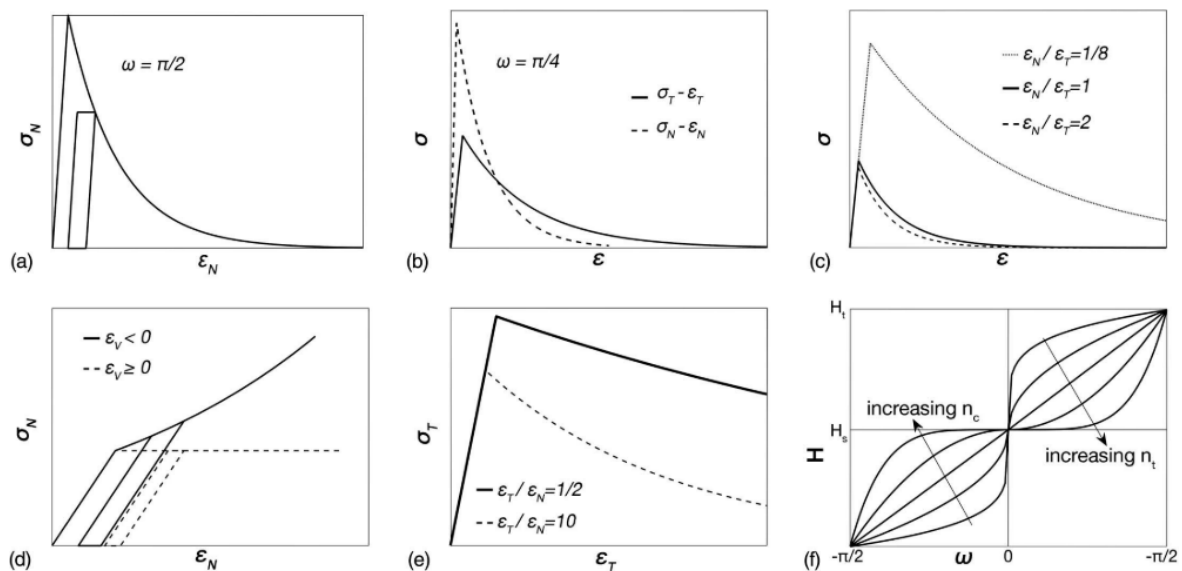
$\dot{\varepsilon}_{\alpha,v}$ is the purely viscous strain rate (Bazant et al. 1997).

$$\dot{\varepsilon}_{\alpha,v} = \xi \kappa \phi S G \sigma_\alpha$$

$\phi = (0.1 + 0.9h^2)\exp(Q_v/R(1/T_0 - 1/T))$
where $Q_v/R \approx 5000^\circ K$.

S is the micro-prestress calculated by solving the differential equation $\dot{S} + \phi_s \kappa S^2 = \kappa_1 [\dot{T} \ln(h) + T \dot{h}/h]$ where $\phi_s = (0.1 + 0.9h^2)\exp(Q_s/R(1/T_0 - 1/T))$ and $Q_s/R \approx 3000^\circ K$.

$\sigma_\alpha = F(\epsilon_\alpha, \eta_\alpha)$, where η_α internal variables of Fascetti et al. (2018)'s constitutive laws:



Lattice Modeling of Mass Transport – Water

Governing equation

$$\frac{\partial \theta}{\partial t} = \frac{\partial}{\partial x} \left(D_w(\theta) \frac{\partial \theta}{\partial x} \right)$$

where D_w is the water diffusion coefficient; θ is the relative water content in concrete.

$$D_w(\theta) = D_0 e^{n\theta}$$

Boundary conditions

$$\theta = \theta_B(t) \quad \text{on } \Gamma_b \in \partial\Omega$$

$$\mathbf{q} = -D_w \frac{\partial \theta}{\partial \mathbf{n}} = \mathbf{q}_B \quad \text{on } \Gamma_q \in \partial\Omega$$

Weak form

$$\begin{aligned} & - \int_{\Omega} \left(D_w(\theta(\mathbf{x}, t)) \nabla N_i(\mathbf{x}) \nabla N_j(\mathbf{x}) \theta(\mathbf{x}, t) \right) d\Omega + \int_{\Omega} N_i(\mathbf{x}) N_j(\mathbf{x}) \frac{\partial \theta(\mathbf{x}, t)}{\partial t} d\Omega \\ & - \int_{\Gamma_q} N_i(\mathbf{x}) \mathbf{q} d\Gamma_q = 0 \end{aligned}$$

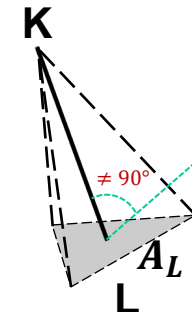
where $N_i(\mathbf{x})$ and $N_j(\mathbf{x})$ are the linear polynomial shape functions.

Discretized weak form

$$\begin{aligned} & - \sum_{j=1}^{n_e} \int_{\Omega^e} \left(D_w(\theta_i(\mathbf{x}, t)) \nabla N_i(\mathbf{x}) \nabla N_j(\mathbf{x}) \right) d\Omega^e \theta_j(t) \\ & + \sum_{j=1}^{n_e} \int_{\Omega^e} N_i(\mathbf{x}) N_j(\mathbf{x}) d\Omega^e \frac{d\theta_j(t)}{dt} - \int_{\Gamma_q^e} N_i(\mathbf{x}) \mathbf{q} \cdot \mathbf{n} d\Gamma_q^e = 0 \quad \forall i = 1, 2, \dots, n^e \end{aligned}$$

Transformation of volume to a line integral

$$\int_{\Omega^e} P(\mathbf{x}) d\Omega^e = \int_{l^e} A_e(\mathbf{x}) P(\mathbf{x}) d\Omega^e$$



Lattice Modeling of Mass Transport – Water (cont.)

Compact form of the discretized weak form

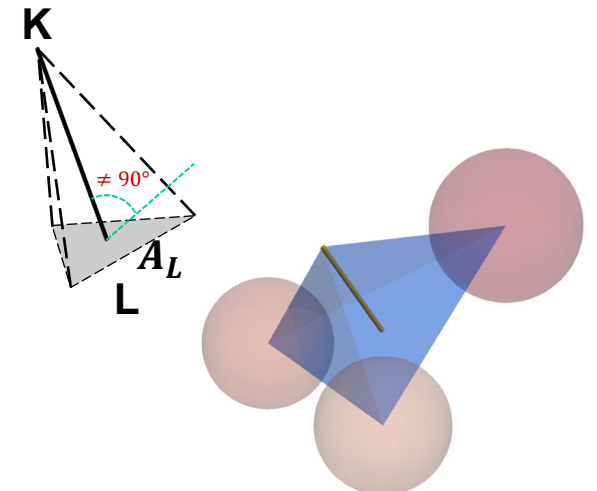
$$\Psi \equiv \mathbf{M} \frac{d\boldsymbol{\theta}}{dt} + \mathbf{K}(\boldsymbol{\theta})\boldsymbol{\theta} - \mathbf{f} = 0$$

where \mathbf{M} is the global mass matrix, \mathbf{h} is the hydraulic head vector, $\mathbf{K}(\mathbf{h})$ is the global diffusion matrix, and \mathbf{f} is the force vector, and where:

$$\mathbf{M}_e = \int_{\Omega^e} \mathbf{N}(\mathbf{x})^T \mathbf{N}(\mathbf{x}) d\Omega^e = \int_{l_e} \xi_V(\mathbf{x}) A_e(\mathbf{x}) \mathbf{N}(\mathbf{x})^T \mathbf{N}(\mathbf{x}) dx = \frac{\xi_2 (1 - v_{ae})^{5/3} A_e^* l_e}{30} \begin{bmatrix} 1 & 1.5 \\ 1.5 & 6 \end{bmatrix}$$

$$\mathbf{K}_e = \int_{\Omega^e} \mathbf{B}^T D_w(\hat{\boldsymbol{\theta}}) \mathbf{B} d\Omega^e = \int_{l_e} D_w(\hat{\boldsymbol{\theta}}) \xi_V(\mathbf{x}) A_e(\mathbf{x}) \mathbf{B}^T \mathbf{B} dx = \frac{\xi_1 (1 - v_{ae}) A_e^*}{3 l_e} \begin{bmatrix} D_w(\theta_1) & -D_w(\theta_1) \\ -D_w(\theta_2) & D_w(\theta_2) \end{bmatrix}$$

$$\mathbf{f}_e = - \int_{\Gamma_q^e} \mathbf{q} \mathbf{N}^T(\mathbf{x}) d\Gamma_q^e = \begin{bmatrix} 0 \\ -q_L \xi_V(\mathbf{x}_L) A_e^* \end{bmatrix}$$



A_e^* is the non-zero cross-sectional area at an endpoint of the transport element, and $A_e(\mathbf{x}) = A_e^*(\mathbf{x} - \mathbf{x}_K) \cdot (\mathbf{x} - \mathbf{x}_K)/l_e^2$ is the cross-sectional area of transport cell with respect to the coordinates of points along the element.

Lattice Modeling of Mass Transport – Water (cont.)

Constitutive law

Crack width dependent hydraulic diffusion (Zhang et al. 2019):

$$D_w(\theta, wc) = \left(D_0 + \gamma \frac{wc^2 pr}{12\eta} \right) e^{n\theta}$$

η is the viscous dynamic coefficient of water and equals 0.001Pa.s.

w_c is the width of the crack that water pass through.

pr is the reference pressure, experimentally determined as 18.6237 N/mm².

γ is an empirical constant that needs to be calibrated by experiments.

Lattice Modeling of Mass Transport – Chloride

Governing equation

$$1 + \lambda(C_f) \frac{\partial C_f}{\partial t} = \boxed{\nabla \cdot (D_{cl}(\theta) \nabla C_f)} + \boxed{C_f \frac{\partial \theta}{\partial t}}$$

Diffusion

Convection

θ is the relative water content in concrete, determined by water transport analysis;
 $\lambda = \partial C_b / \partial C_f$ is the chloride binding capacity, which depends on the free chloride concentration C_f .

$$\lambda = 10^B \frac{A_0 \beta_{gel}}{35450 \beta_{sol}} \left(\frac{C_f}{35.45 \beta_{sol}} \right)^{A-1}$$

Lattice Modeling of Mass Transport – Chloride (cont.)

Discretized weak form

$$\begin{aligned}
 & -\sum_{j=1}^{n_e} \left(\int_{\Omega^e} \left(D_{cl}(\theta_i) \nabla N_i(\mathbf{x}) \nabla N_j(\mathbf{x}) + \frac{d\theta_i}{dt} N_i(\mathbf{x}) N_j(\mathbf{x}) \right) d\Omega^e C_{f,j}(t) + \sum_{j=1}^{n_e} \int_{\Omega^e} (1 + \lambda(C_{f,i})) N_i(\mathbf{x}) N_j(\mathbf{x}) d\Omega^e \frac{dC_{f,j}(t)}{dt} \right. \\
 & \quad \left. - \int_{\Gamma_q^e} N_i(\mathbf{x}) \mathbf{p} \cdot \mathbf{n} d\Gamma_q^e = 0 \right) \quad \forall i = 1, 2, \dots, n^e
 \end{aligned}$$

where $\mathbf{p} = -D_{cl}(\theta) \frac{\partial C_f}{\partial \mathbf{n}}$.

Compact form of the discretized weak form

$$\Psi \equiv \mathbf{M} \frac{d\boldsymbol{\theta}}{dt} + \mathbf{K}(\boldsymbol{\theta}) \boldsymbol{\theta} - \mathbf{f} = 0$$

$$\mathbf{K}_e = \int_{\Omega^e} \left(\mathbf{B}^T D_{cl}(\hat{\theta}) \mathbf{B} + \frac{\partial \hat{\theta}}{\partial t} \mathbf{N}(\mathbf{x})^T \mathbf{N}(\mathbf{x}) \right) d\Omega^e = \int_{l_e} \xi_V(\mathbf{x}) A_e(\mathbf{x}) \left(D_{cl}(\hat{\theta}) \mathbf{B}^T \mathbf{B} + \frac{\partial \hat{\theta}}{\partial t} \mathbf{N}(\mathbf{x})^T \mathbf{N}(\mathbf{x}) \right) d\mathbf{x} = \frac{\xi_1(1 - v_{ae}) A_e^*}{3l_e} \begin{bmatrix} D_{cl}(\theta_1) & -D_{cl}(\theta_1) \\ -D_{cl}(\theta_2) & D_{cl}(\theta_2) \end{bmatrix} + \frac{\xi_2(1 - v_{ae})^{5/3} A_e^* l_e}{30} \begin{bmatrix} \frac{\partial \theta_1}{\partial t} & 1.5 \frac{\partial \theta_1}{\partial t} \\ 1.5 \frac{\partial \theta_2}{\partial t} & 6 \frac{\partial \theta_2}{\partial t} \end{bmatrix}$$

$$\mathbf{M}_e = \int_{\Omega^e} (1 + \lambda(\widehat{C}_f)) \mathbf{N}(\mathbf{x})^T \mathbf{N}(\mathbf{x}) d\Omega^e = \int_{l_e} \xi_V(\mathbf{x}) A_e(\mathbf{x}) \mathbf{N}(\mathbf{x})^T \mathbf{N}(\mathbf{x}) d\mathbf{x} = \frac{\xi_2(1 - v_{ae})^{5/3} A_e^* l_e}{30} \begin{bmatrix} 1 + \lambda(C_{f,1}) & 1.5(1 + \lambda(C_{f,1})) \\ 1.5(1 + \lambda(C_{f,2})) & 6(1 + \lambda(C_{f,2})) \end{bmatrix}$$

$$\mathbf{f}_e = - \int_{\Gamma_q^e} \mathbf{p} \mathbf{N}^T(\mathbf{x}) d\Gamma_q^e = \begin{bmatrix} 0 \\ -p_L \xi_V(\mathbf{x}_L) A_e^* \end{bmatrix}$$



Lattice Modeling of Mass Transport – Chloride (cont.)

Constitutive law

Crack width dependent chloride diffusion coefficient (Saeki and Niki 1996; Djerbi et al. 2008)

$$D_{cl}(\theta, wc) = \begin{cases} D_{cl} 0.0032 \times 10^{2.5\theta} & wc = 0 \mu m \\ D_{cl} & wc < \frac{D_{cl} + 2 \times 10^{-10}}{2 \times 10^{-11}} \mu m \\ 2 \times 10^{-11} \times wc - 2 \times 10^{-10} & \frac{D_{cl} + 2 \times 10^{-10}}{2 \times 10^{-11}} \mu m \leq wc \leq 80 \mu m \\ 14 \times 10^{-10} & wc > 80 \mu m \end{cases}$$

D_{cl} is the chloride diffusivity in the saturated state.

Numerical Solution Procedure – Mechanical

A dynamic explicit method with central difference is applied

$$\mathbf{M}\ddot{\mathbf{Q}} + \mathbf{K}\mathbf{Q} = \mathbf{R}$$

Central difference leads to

$$\left(\frac{1}{\Delta t^2}\mathbf{M}\right)\mathbf{Q}^{t+\Delta t} = \hat{\mathbf{R}}^t = \mathbf{R}^t - \left(\mathbf{K} - \frac{2}{\Delta t^2}\mathbf{M}\right)\mathbf{Q}^t - \left(\frac{1}{\Delta t^2}\mathbf{M}\right)\mathbf{Q}^{t-\Delta t}$$

The mass matrix \mathbf{M} is diagonalized by simply discarding the off-diagonal terms, then

$$Q_i^{t+\Delta t} = \boxed{\hat{R}_i^t} \left(\frac{\Delta t^2}{m_{ii}} \right)$$

Residual force

As with other explicit methods, the \mathbf{K} matrix is not necessary to evaluate since

$$\mathbf{K}\mathbf{Q}^t = \sum_i \mathbf{K}^{(i)}\mathbf{Q}^t = \sum_i \mathbf{F}^{(i),t}$$

Numerical Solution Procedure – Mechanical (cont.)

A dynamic explicit method with central difference is applied

When calculating \mathbf{F}^t ,

$$\varepsilon_{\alpha,v}^t = \varepsilon_{\alpha,v}^{t-\Delta t} + \Delta t \xi \kappa \phi S^t G \sigma_{\alpha}^{t-\Delta t}$$

Where $S^t = S^{t-\Delta t} - \phi_s \kappa (S^{t-\Delta t})^2 \Delta t + \kappa_1 [\Delta T \ln(h) + T \Delta h / h]$.

Then the Residual force is

$$\widehat{\mathbf{R}}^t = \mathbf{R}^t - \sum_i \mathbf{F}^{(i),t} - \left(\frac{1}{\Delta t^2} \mathbf{M} \right) (\mathbf{Q}^{t-\Delta t} - 2\mathbf{Q}^t)$$

Stability criterion

$$\Delta t < 2/\omega_{max},$$

ω_{max} is the highest natural frequency

$$\det(\mathbf{K} - \omega^2 \mathbf{M}) = 0$$

Numerical Solution Procedure – Transport

A Crank-Nicolson method and Newton-Raphson solver for semi-implicit dynamic integration is applied

Temporal discretization utilizing Crank-Nicolson method:

$$\left(\mathbf{M} + \frac{1}{2} \mathbf{K}^{n+1} \Delta t \right) \mathbf{h}^{n+1} = \left(\mathbf{M} - \frac{1}{2} \mathbf{K}^n \Delta t \right) \mathbf{h}^n + \frac{1}{2} (\mathbf{f}^{n+1} + \mathbf{f}^n)$$

$$\mathbf{h} = \{\boldsymbol{\theta}; \mathbf{C}_f\}$$

Due to spurious oscillations in the solution of transient problems, the **maximum time step** is constrained to

$$\Delta t = \frac{l_{min}^2}{2D_{max}}$$

where l_{min} is the minimum value of the lattice element length in the mesh and D_{max} is the largest transport coefficient throughout the simulation.

Numerical Solution Procedure – Transport (cont.)

A Crank-Nicolson method and Newton-Raphson solver for semi-implicit dynamic integration is applied

Newton-Raphson iterations

$$\left(\mathbf{M} + \frac{1}{2} \mathbf{K}^{n+1} \Delta t \right) \mathbf{h}^{n+1} = \boxed{\left(\mathbf{M} - \frac{1}{2} \mathbf{K}^n \Delta t \right) \mathbf{h}^n + \frac{1}{2} (\mathbf{f}^{n+1} + \mathbf{f}^n)}$$

\downarrow

$R(\mathbf{h})$

$$\mathbf{h}^{n+1} = \mathbf{h}^n + \Delta \mathbf{h}$$

$$R(\mathbf{h}^n) + \frac{\partial R(\mathbf{h}^n)}{\partial \mathbf{h}} \Delta \mathbf{h} = R(\mathbf{h}^{n+1})$$

where

$$\frac{\partial R(\mathbf{h})}{\partial \mathbf{h}} = \left(\mathbf{M}(\mathbf{h}) + \frac{1}{2} \Delta t \mathbf{K}(\mathbf{h}) \right) + \left(\frac{\partial \mathbf{M}(\mathbf{h})}{\partial \mathbf{h}} + \frac{1}{2} \Delta t \frac{\partial \mathbf{K}(\mathbf{h})}{\partial \mathbf{h}} \right) \mathbf{h}$$



Numerical Solution Procedure – Transport (cont.)

A Crank-Nicolson method and Newton-Raphson solver for semi-implicit dynamic integration is applied

For the water transport problem,

$$\frac{\partial \mathbf{M}(\mathbf{h})}{\partial \mathbf{h}} = \mathbf{0}$$

$\frac{\partial \mathbf{K}(\mathbf{h})}{\partial \mathbf{h}} = \mathbf{K}_T$ is a third-order tensor, with

element-level components

$$K_{Te111} = \frac{\xi_1(1-\nu_{ae})A_e^*}{3L_e} D'_w(h_1)$$

$$K_{Te121} = -\frac{\xi_1(1-\nu_{ae})A_e^*}{3L_e} D'_w(h_1)$$

$$K_{Te211} = 0$$

$$K_{Te221} = 0$$

$$K_{Te112} = 0$$

$$K_{Te122} = 0$$

$$K_{Te212} = -\frac{\xi_1(1-\nu_{ae})A_e^*}{3L_e} D'_w(h_2)$$

$$K_{Te222} = \frac{\xi_1(1-\nu_{ae})A_e^*}{3L_e} D'_w(h_2)$$

where $D'_w(h)$ is the first derivative of $D_w(h)$ and

$$\mathbf{K}_{Te}\mathbf{h}_e = \begin{bmatrix} K_{Te111}h_1 + K_{Te112}h_2 & K_{Te121}h_1 + K_{Te122}h_2 \\ K_{Te211}h_1 + K_{Te212}h_2 & K_{Te221}h_1 + K_{Te222}h_2 \end{bmatrix}$$

Numerical Solution Procedure – Transport (cont.)

A Crank-Nicolson method and Newton-Raphson solver for semi-implicit dynamic integration is applied

For the **chloride** transport problem,

$$\frac{\partial \mathbf{K}(\mathbf{h})}{\partial \mathbf{h}} = \mathbf{0}$$

$\frac{\partial \mathbf{M}(\mathbf{h})}{\partial \mathbf{h}} = \mathbf{M}_T$ is a third-order tensor, with element-level components

$$M_{Te111} = \frac{\xi_2(1-\nu_{ae})^{5/3} A_e^* L_e}{30} \lambda'(C_{f,1})$$

$$M_{Te121} = \frac{\xi_2(1-\nu_{ae})^{5/3} A_e^* L_e}{20} \lambda'(C_{f,1})$$

$$M_{Te211} = 0$$

$$M_{Te221} = 0$$

$$M_{Te112} = 0$$

$$M_{Te122} = 0$$

$$M_{Te212} = \frac{\xi_2(1-\nu_{ae})^{5/3} A_e^* L_e}{20} \lambda'(C_{f,2})$$

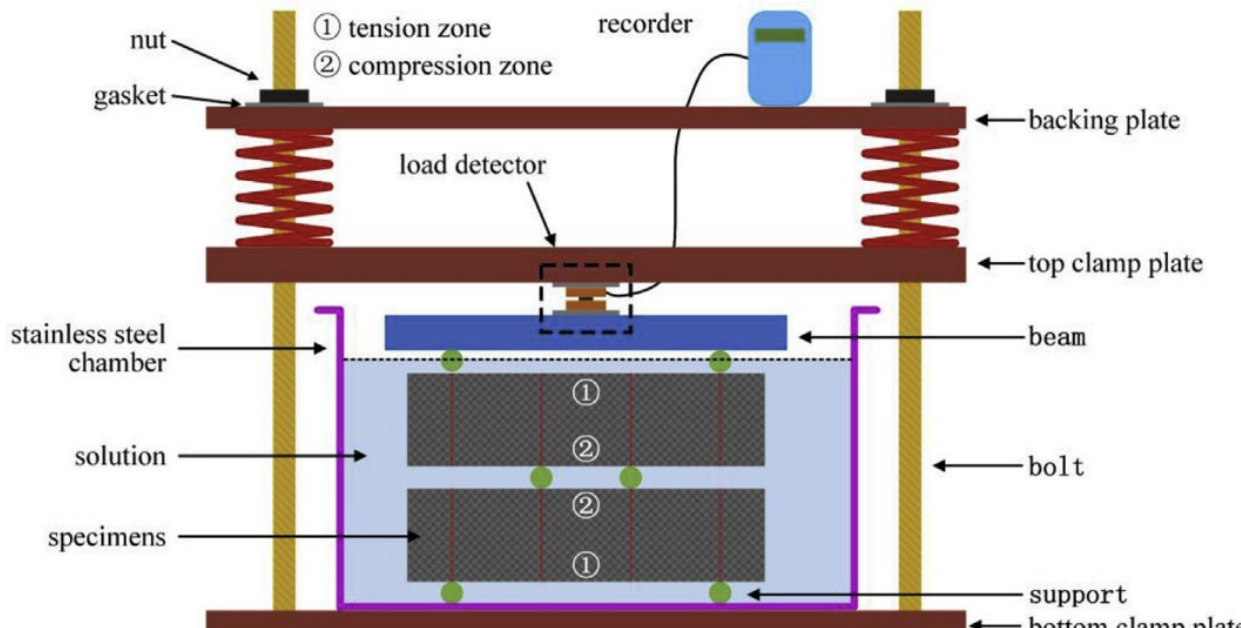
$$M_{Te222} = \frac{\xi_2(1-\nu_{ae})^{5/3} A_e^* L_e}{5} \lambda'(C_{f,2})$$

where $\lambda'(h)$ is the first derivative of $\lambda(h)$ and

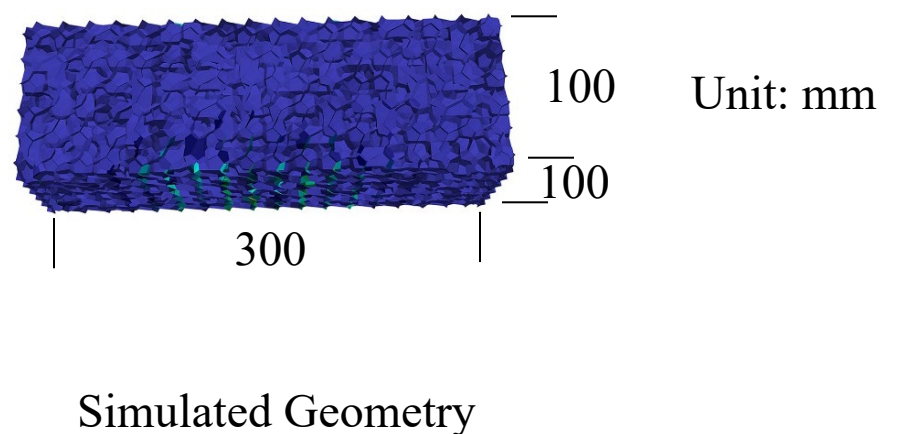
$$\mathbf{M}_{Te} \mathbf{h}_e = \begin{bmatrix} M_{Te111} h_1 + M_{Te112} h_2 & M_{Te121} h_1 + M_{Te122} h_2 \\ M_{Te211} h_1 + M_{Te212} h_2 & M_{Te221} h_1 + M_{Te222} h_2 \end{bmatrix}$$

Preliminary Results

**Chloride immersion test of plain concrete beam under 4-point bending
(Wang et al. 2019)**

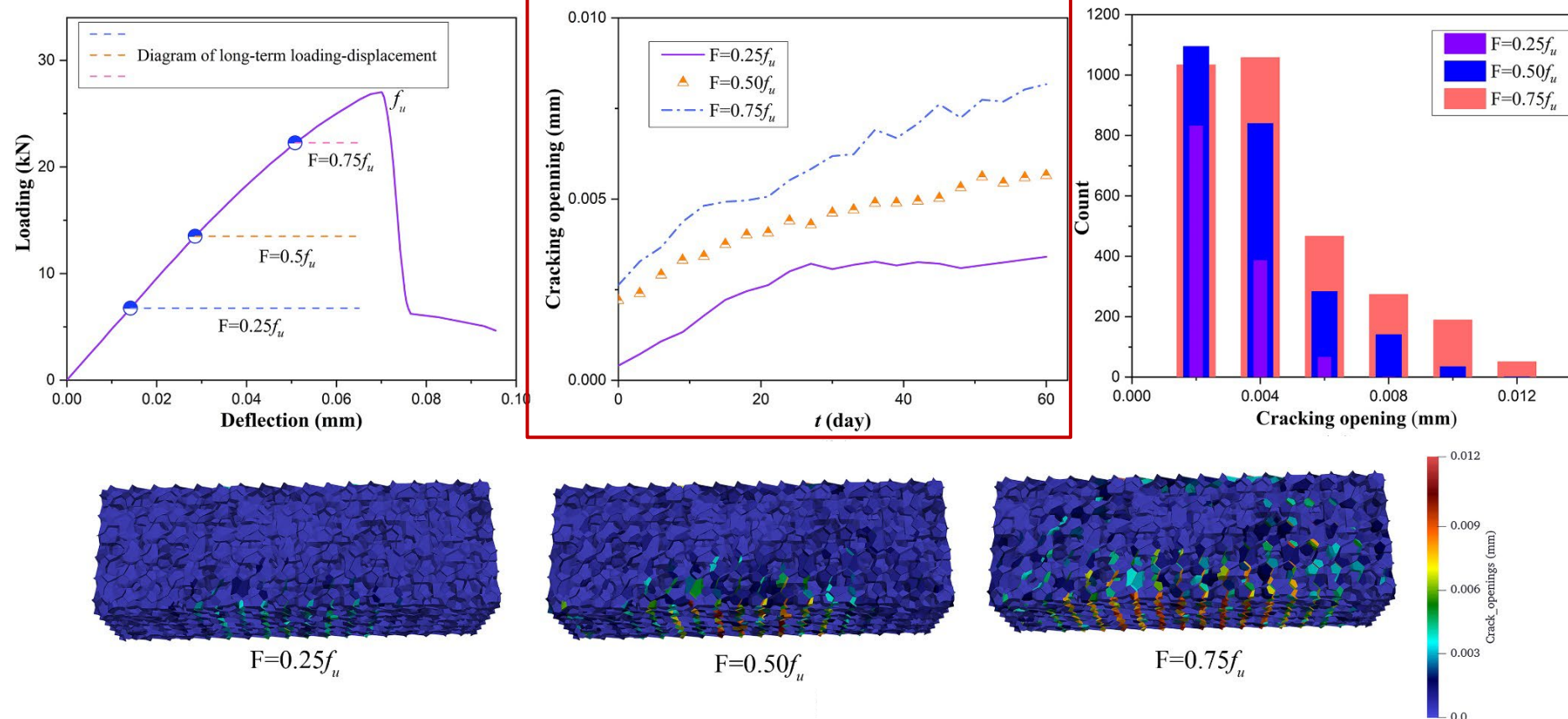


Experimental setup



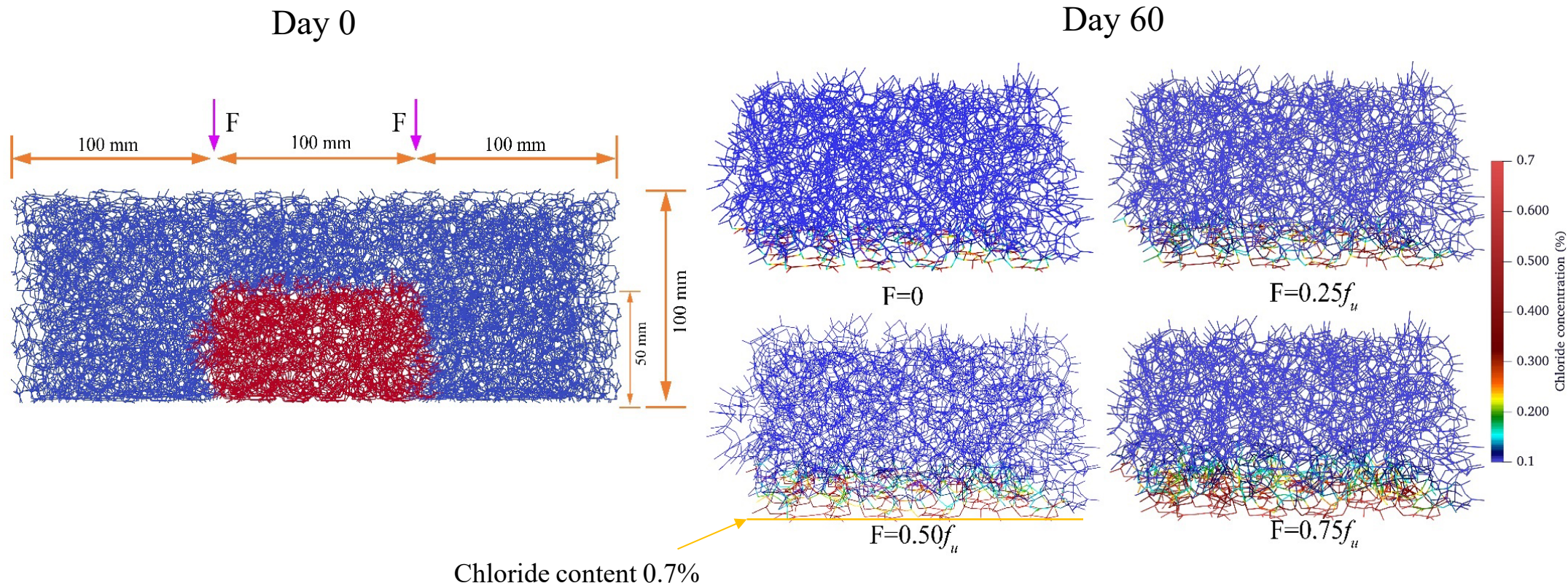
Preliminary Results (cont.)

Mechanical results



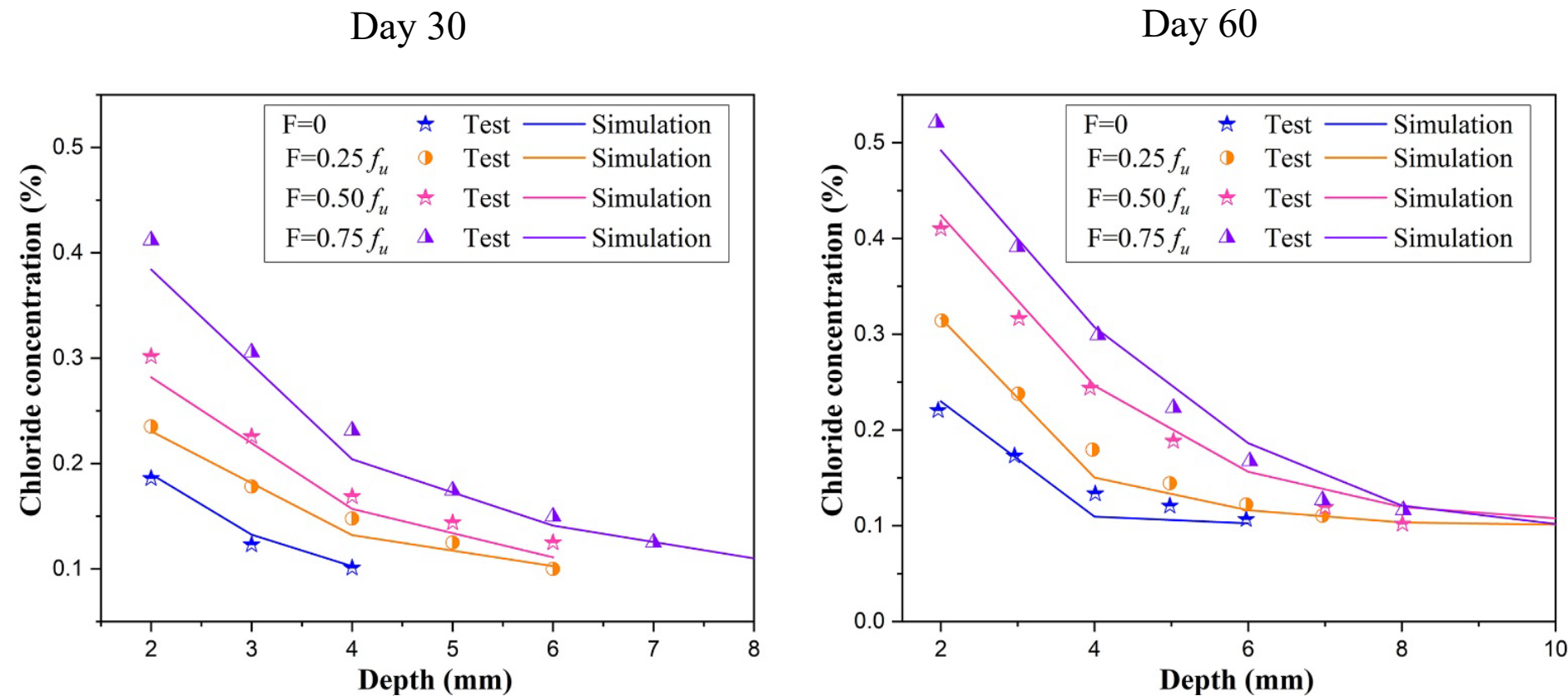
Preliminary Results (cont.)

Transport results – simulation



Preliminary Results (cont.)

Transport results – validation



Conclusions

1. An **integrated nonlinear framework** for fracture, mass transport, and creep simulations is formulated.
2. A **dynamic solution strategy for this coupled model** is proposed using central difference, forward difference, the Crank-Nicolson method and the Newton-Raphson method .
3. **Preliminary application** of this model **demonstrates its ability** to accurately estimate chloride transport process in unsaturated concrete subjected to long-term loading.



References

1. Jia, D., Brigham, J. C., & Fascetti, A. (2024). An efficient static solver for the lattice discrete particle model. *Computer-Aided Civil and Infrastructure Engineering*, accepted.
2. Fascetti, A., Bolander, J. B., & Nisticò, N. (2018). Lattice discrete modeling of concrete under compressive loading: Multiscale experimental approach for parameter determination. *Journal of Engineering Mechanics*, 8(144).
3. Cusatis, G., Pelessone, D., & Mencarelli, A. (2011). Lattice discrete particle model (LDPM) for failure behavior of concrete. I: Theory. *Cement and Concrete Composites*, 33(9), 881-890.
4. Cibelli, A., Di Luzio, G., & Ferrara, L. (2023). Numerical simulation of the chloride penetration in cracked and healed UHPC via a discrete multiphysics model. *Journal of Engineering Mechanics*, 149(12), 05023001.
5. Qiu, Q., & Dai, J. G. (2021). Meso-scale modeling of chloride diffusivity in mortar subjected to corrosion-induced cracking. *Computer-Aided Civil and Infrastructure Engineering*, 36(5), 602-619.
6. Abdellatef, M., Boumakis, I., Wan-Wendner, R., & Alnaggar, M. (2019). Lattice Discrete Particle Modeling of concrete coupled creep and shrinkage behavior: A comprehensive calibration and validation study. *Construction and Building Materials*, 211, 629-645.
7. Bažant, Z. P., Hauggaard, A. B., Baweja, S., & Ulm, F. J. (1997). Microprestress-solidification theory for concrete creep. I: Aging and drying effects. *Journal of Engineering Mechanics*, 123(11), 1188-1194.
8. Zhang, Y., Zhang, S., Wei, G., Wei, X., Jin, L., & Xu, K. (2019). Water transport in unsaturated cracked concrete under pressure. *Advances in Civil Engineering*, 2019(1), 4504892.
9. Saeki, T., and Niki, H. (1996). Migration of chloride ions in non-saturated mortar. *Proc. Jap. Concr. Inst.*, 18(1), 963–968 (in Japanese).
10. Wang, J., Niu, D., Wang, Y., He, H., & Liang, X. (2019). Chloride diffusion of shotcrete lining structure subjected to nitric acid, salt–frost degradation, and bending stress in marine environment. *Cement and Concrete Composites*, 104, 103396.
11. Djerbi, A., Bonnet, S., Khelidj, A., & Baroghel-Bouny, V. (2008). Influence of traversing crack on chloride diffusion into concrete. *Cement and Concrete Research*, 38(6), 877-883.

Acknowledgements

- John C. Brigham, Alessandro Fascetti, Yingbo Zhu
- The Impactful Resilient Infrastructure Science and Engineering (IRISE) Consortium

